Beamforming of Lamb Waves using 2D Arrays: A Comparative Study

T. STEPINSKI, L. AMBROZIŃSKI AND T. UHL

ABSTRACT

Structural health monitoring (SHM) of plate-like structures can be performed using 2D array of transducers. An optimal array topology as well as an efficient beamforming scheme becomes essential when designing a beamformer based on 2D arrays. In this paper we consider both aspects of the beamforming design process. We outline a consistent methodology including theoretical, numerical and experimental investigation of a diversity of 2D array topologies in application to the beamforming of LWs. We compare a number of symmetrical 2D topologies forming circular, star-like and square patterns. In the second part we propose and analyze multi-static beamformers with sparse transmission apertures and compare their performance with classical beamformer based on the mono-static phased array approach.

INTRODUCTION

Structural health monitoring (SHM) of plate-like structures is a hot topic of research since many such constructions must meet high safety standards. Lamb waves (LW) are a promising tool for these applications since thanks to their ability to propagate over long distances and sensitivity to various types of damages [1]. The sensitivity of a SHM system can be enhanced by means of active ultrasonic phased arrays (PA) due to their superior signal to noise-ratio and beam-steering capability [2]. It appeared, however, that 2D array topologies are required for unequivocal damage localization in the SHM of plate-like structures. [2]. Therefore, a number of reports has been published concerning various shapes of those arrays, for instance, star [3], square [4], circular [5] and spiral [6] shaped arrays.

The quality of an image created using an array of a defined topology depends also, among other factors, on the array's aperture and imaging technique used. Moving transducers have been used in the mechanized NDT applications to increase array's aperture by means of synthetic aperture focusing technique (SAFT) [7,8]. Since this solution would be infeasible in most SHM applications,

T. Stepinski, Ł. Ambroziński, T. Uhl, AGH University of Science and Technology, al. Mickiewicza 30, 30-059 Kraków, Poland; tstepin@agh.edu.pl

this paper is concerned with 2D static arrays that are permanently attached to the monitored structure. These arrays can take advantage of multiple emitting transducers capable of illuminating defect from diverse locations and directions, which results in an extension of array's effective aperture [9].

Another critical factor that affects the performance of a PAs-based SHM system is signal processing technique implemented in the beamforming scheme. The most common scheme used for processing snapshots captured by an array, mostly due to its simplicity and robustness, employs the delay and sum (DAS) operations in time domain. More advanced methods able to improve angular [10] and radial resolution [11,12] can also be implemented to the Lamb waves sensed using PAs. However, advanced processing techniques require precise information concerning material properties, which can create limitations in practical applications, especially, for anisotropic materials.

In this paper novel methods for LWs imaging are discussed. The techniques are based on multistatic synthetic aperture focussing (MSAF) approach, which assumes that signal acquisition is performed using sparse transmit and receiving arrays. Comparing to full matrix MSAF approach the proposed methods require simpler hardware and lower computation power for processing ultrasonic data, which is particularly important in SHM applications.

THEORETICAL BACKGROUND

Application of array technique to SHM of plate-like structures involves a set of transducers that are permanently attached to, or embedded into the structure to enable performing inspection of a large region of interest (ROI) from a fixed location. The imaging schemes can be roughly divided into two categories, the phased array (PA) and the synthetic focusing (SF) techniques.

If an array is used in an active PA mode, the transmitting and receiving sub-arrays consist normally of the same elements. These elements are excited in transmission by the time-shifted pulses to obtain a steered wavefront in order to physically focus the beam energy in the desired point in the ROI. The scattered waves are received by the same elements in the reception mode and amplified by introducing respective time delays bringing the received pulses in phase. Beamformers implementing DAS technique are commonly used in ultrasound applications. Using a steered and possibly focused beam improves angular (azimuth) resolution in ultrasonic image but it requires scanning of the whole ROI in many point. This means that the send-receive cycle has to be repeated for a number of azimuths and ranges within the ROI, which results in a low acquisition speed.

Alternatively to the PA, the SF techniques, performing focusing after the data acquisition, can be used. In these methods, the image is formed by successive excitation of transmuting elements and reception of the scattered waves by the sensing array elements. The number of measurement cycles is at most equal to the number of array's elements, therefore, if uniform focus in ROI is needed the SF techniques require lower number of excitations and offer higher acquisition speed than PA.

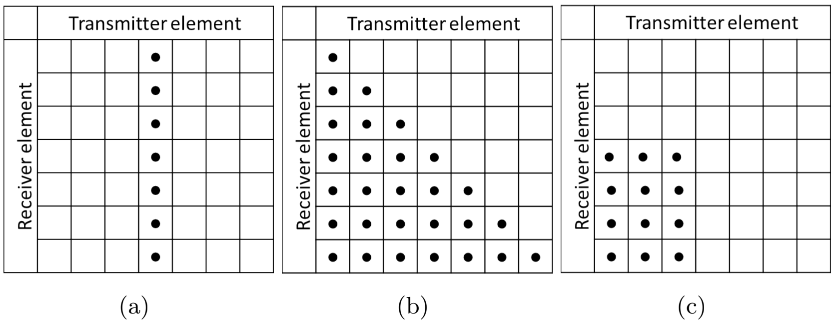

Figure 1. Transmit-receive geometries of SF algorithms: mono-static STMR a) TFM b) MSAF c).

Generally, various transmit-receiver combinations can be used. In the common source method [13], presented in Figure 1a, a single transmitter and multiple receivers (STMR) are used. For N element array, this technique requires only one firing and N synchronized input channels.

It appears, however, that performance of an array with given topology can be improved using different combinations of transmit-receive elements. Illuminating a target from numerous positions means that the array's aperture is distributed and imaging is performed synthetically. The SA technique is in general superior to the STMR approach. The performance of both techniques can be compared in the terms of the *effective array aperture*, which is defined as en equivalent receive aperture that would produce a radiation pattern identical to the convolved transmit-receive setup if only a single point source was used for the transmission [14].

For an array with N elements a full matrix of N^2 transmit-receive data can be acquired if all the elements are fired in N transmission cycles. The full matrix processing, which relies on the SF in the all points in the ROI, is known as total focusing method (TFM), [9]. Due to the reciprocity, however, the resulting matrix will be symmetrical, therefore the number of transmit-receive cycles can be limited according to Figure 1b.

There are, however, many other ways of acquiring data for the SF processing that depend on array's topology and the setup of the transmitting aperture. Most of these ways are designed to reduce number of transmissions with minor loss of resolution and an acceptable signal to noise ratio. Generally, this can be achieved by using sparse transmitting apertures. If elements of a sparse transmitting aperture are distributed across the full aperture of the array, there will be no loss in the field of view and only a minor loss in lateral resolution.

The MSAF approach, which will be considered here and illustrated by Figure 1 uses different transmitting and sensing elements. Moreover, it is assumed that single transducers are not used in the pulse-echo mode in a single cycle, which allows for significant simplification of the hardware used for data acquisition. Since the amount of data subject to processing is reduced (which can be seen from the comparison of figs 1b and 1c) the algorithm implementation requires lower computational power than the TFM and only minor drop of performance is expected. A more detailed description of the technique can be found in [15].

EXAMPLES of IMAGING SCHEMES

Beampattern evaluation is performed normally assuming a monochromatic, continuous wave excitation. In SHM applications, however, tone-burst or broadband pulses are used to enable damage localization by the time of flight extraction of the damage-related reflections. Since the shape of the excitation signal plays a vital role in the mechanism of Lamb wave propagation and their beamforming, in this section simulations of Lamb wave propagation for broadband excitation signals will be presented. The responses processed with beamforming algorithms will be used to present and discuss performance of the selected 2D arrays.

Dispersive and multimodal nature of Lamb waves can be investigated using the relation between the phase velocity and the product of the plate thickness and excitation frequency given by the numerical solution of Rayleigh-Lamb equation. When the dispersion curves are available it is possible to evaluate the response of the structure due to the defined excitation using frequency-dependent system transfer function (STF) [16].

The STF method was used for generating dispersive signals in the simulations of LW propagation in a 2 mm thick aluminum plate (below, these results will be referred to as theoretical). In the setups presented below a set of point-like transducers arranged in regular 2D arrays, acting as transmitters or receivers, was assumed and a point-like scatterer was localized in the array's far-field. In the simulations of wave propagation, based on the STF approach, the length of the propagation path was equal to the transmitter-scatterer-receiver distance. Single mode excitation was used to focus on the dispersion phenomenon and the multimodal nature of the LWs was not considered.

Evaluation of array's shape in monostatic mode

Below, various topologies presented in Figure 2 will be discussed to illustrate the influence of array topology on beamforming. All analyzed arrays consist of 32 sensors and a single transmitter is placed in the center of each array.

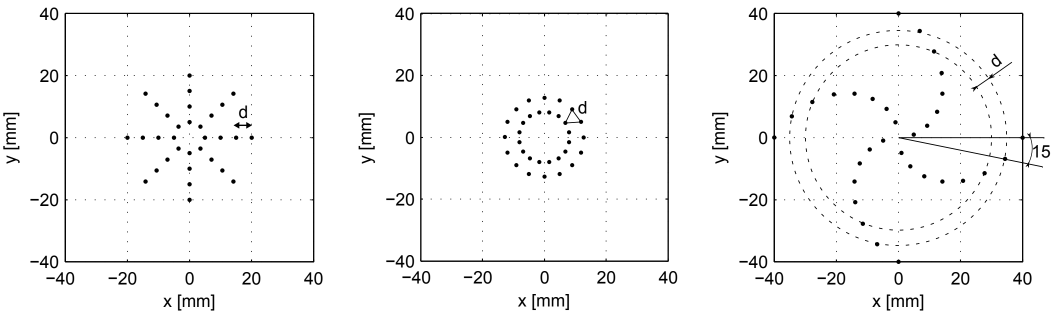

(a) (b) (c)

Figure 2. Investigated array topologies: (a) star-shaped, (b) circular, (c) spiral. Note that constant element number and pitch results in the different aperture size.

All investigated topologies have at least 2 axes of symmetry, therefore theoretical evaluation of the beampatterns can be limited to the range of $0° - 90°$ and mirrored for the remaining directions.

The methodology presented in our previous work [17] was used to obtain the theoretical, numerical and experimental signals. The numerical simulations were performed using our LISA tool and the experiments were performed using laser scanning vibrometer. An example of beampatterns obtained using those methods can be seen in Figure 3a, b, c, respectively for spiral, circular and star-shaped array, and for an incident plane wave with an arbitrary selected incident angle of 60°. Good agreement of the directivity characteristics obtained theoretically, numerically and experimentally can be observed for all of the topologies, however, the experimental beampatterns are better reproduced by the simulated results than the theoretical ones. It can be explained by the fact that LISA is a more accurate method for modeling of Lamb waves propagation than the theoretical approach based on the simplified STF model.

The beampatterns obtained for the waves with incident angle in the range of $0° - 90°$ were analyzed and the selected parameters estimated from the characteristics were presented in our previous paper [17]. Main lobe width was estimated and the maximal and minimal values of lobe width as well as the highest and the lowest sidelobe levels were investigated. The results show that the spiral array has the narrowest main lobe among the investigated topologies, which was expected since this array has the largest aperture. However, the spiral-shaped array presented a significant side-lobes level. The circular array presented almost constant properties for different angles, however, its performance was poor due to small aperture. Therefore a star-shaped array was selected for the further analysis as a compromise between the performance and simplicity.

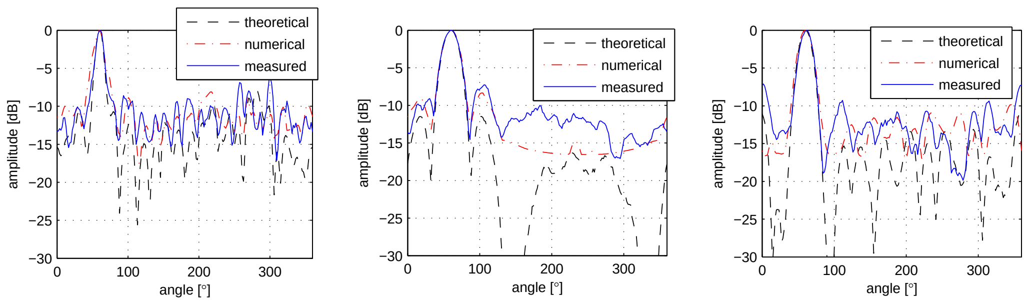

(a) (b) (c)

Figure 3. Beampatterns evaluated for the wave with incident angle 60° for: (a) spiral, (b) circular and (c) star-shaped array. The theoretical profiles were obtained using the STF approach while the numerical ones by means of LISA simulation.

Multistatic imaging

In the simulation which follows the SA concept will be illustrated in the MSAF setup consisting of multiple transmitters and multiple receivers (MTMR) implemented in the form of star-shaped array of transmitters/receivers presented in Figure 2a. The elements from the horizontal, linear sub-array were used as transmitters whereas the transducers in the remaining arms were used as sensors. A point-like scatterer was localized at a distance of 250 mm at an angle of 110° from the array. The simulated responses from the each transmitter-receiver pair formed a matrix consisting of 8x24 time-traces. The snapshots were processed using DAS algorithm and the resulting image is presented in Figure 4b.

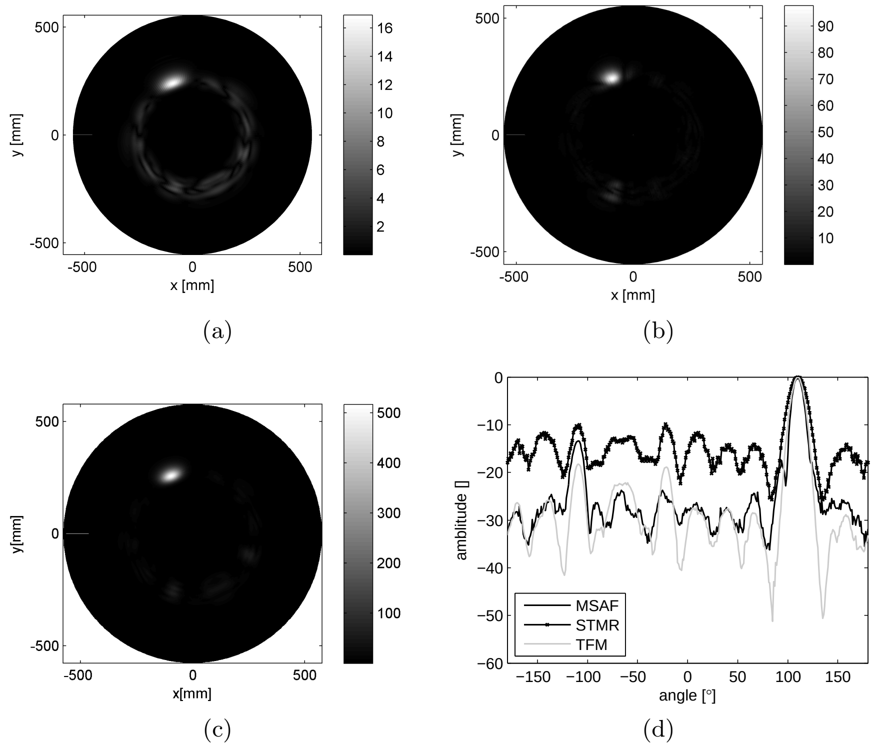

Figure 4. Target image obtained using the star-like setup. STMR a), MSAFT b), TFM c). Comparison of the beampattern resulting for STMR, MSAF, TFM d). The profiles plotted in panel c were obtained using the STF method.

Comparing this image to that presented in Figure 4a, obtained using the same array operating in the STMR mode, can be easily seen that, although the same topology of the array and the same number of elements were used, the MSAF method yields a considerably improved result. A full matrix of 32x32 time-traces was processed using the TFM in the final simulation. Comparing the resulting image, presented in Figure 4c, to the MASF result from Figure 4b shows a slight improvement in the quality of TFM image.

In order to investigate the differences between the images, the results were processed to find maxima occurring at the successive azimuths, the resulting beampatterns are presented in Figure 4d. Comparison of the results shows that the multistatic approach is superior to the monostatic one in terms of main lobe width and range resolution. The best result in terms of side-lobe levels was obtained using TFM, however, in the presented case the MSAF exhibited the narrowest main lobe.

Imaging using an active transmitting array

In the next series of the MTMR simulations the star shaped array, presented in Figure 2a, was used in sweeping PA mode. In this mode the elements of the horizontal transmitting array were fired using time-shifted signals to form a plane wave sweeping the ROI. The backscattered signals were received by the remaining star arms and post-processed to obtain a high resolution image. In other words, focusing in the transmission was done in the material and focusing in the reception was performed off-line by the DAS operation of the captured snapshots.

In the presented simulation, azimuth of a far-field point-like scatterer was, like previously, 110°. Since the transmitting array was linear and it produced a mirrored lobe, the transmission angle was limited to the range 0 – 180° but various angular sweeping steps were considered. In the first step the beam was transmitted at a set of azimuths with the step of 10°, which lead to the 19x24 matrix of time-traces (19 azimuths and 24 receiving elements). The same resolution was used to process the acquired snapshots, the result can be seen in Figure 4a. Next, the same data was processed with 1° resolution both in the transmission and reception resulting in 181x24 matrix of time-traces (181 azimuths and 24 receiving elements); the results are presented in Figure 5b. Comparison of the images shown in Figure 5a and b shows that rather poor resolution obtained for the 10° step can be improved if the captured data is processed with a higher resolution in the reception and a smaller step in the transmission is used simultaneously.

The beampatterns obtained for the images from Figure 5b and Figure 4b can be compared in Figure 5c. From the plots it can be seen that both approaches, the synthetic MSAF focusing and the PA sweeping, yield essentially the same result.

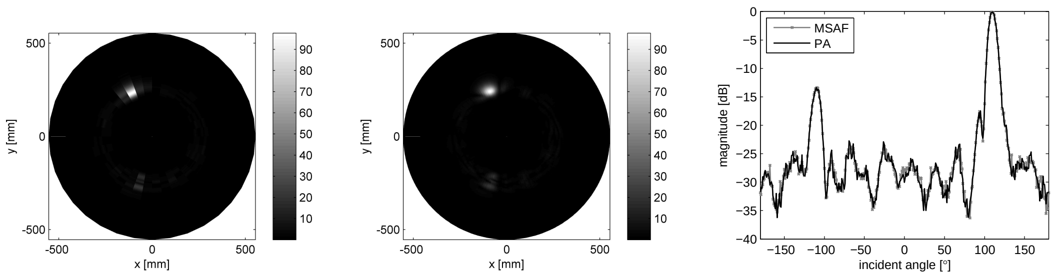

(a) (b) (c)

Figure 5. Target images obtained in the STF simulations of the PA mode for the following emission/reception sweeping steps: 10°/10° a), 1°/1°b). The beampatterns obtained using the MSAF and the MTMR-PA mode with azimuth sweeping step 1°/1° c).

CONCLUSIONS

Various approaches to beamforming of Lamb waves were presented in the paper; multistatic synthetic aperture focusing technique was compared to the monostatic and the total focusing method.

Based on the results, can be concluded that the multistatic and total focusing approaches take an advantage of multiple successive transmissions, which allows to illuminate targets from a set of diverse positions and results in a high quality produced image. Application of this technique enables obtaining narrower main-lobe and lower side-lobes level comparing to the monostatic setup using the same array topology.

It was shown in the simulations that focusing can be performed partially in the inspected structure with the use of an active transmitting array operating in the PA mode. However, a large number of transmission-reception cycles is required to achieve high image resolution in this mode. Moreover, this mode requires a multiple channel system capable of simultaneous generation of time-shifted signals while in the multistatic setup a single, multiplexed output channel is sufficient. Therefore the multistatic synthetic aperture approach, in which the data can be acquired by means of a relatively simple hardware and subsequently processed off-line with an arbitrary resolution, is superior to the active scheme in the SHM applications.

REFERENCES

1. A. Raghavan and C. E. S. Cesnik, "Review of guided-wave structural health monitoring," *The Shock and Vibration Digest* **39**, p. 91114, March 2007.
2. V. Giurgiutiu, *Structural Health Monitoring With Piezoelectric Wafer Active Sensors*, Academic Press, New York, 2008.
3. L. Ambrozinski, T. Stepinski, and T. Uhl, "Self focusing of 2D arrays for SHM of plate-like structures using time reversal operator," in *Structural Health Monitoring Condition-Based Maintenance and Intelligent Structures*, F.-K. Chang, ed., p. 11191127, DEStech Publications, Inc., cop, (Stanford, USA), September 1315 2011.
4. M. Engholm and T. Stepinski, "Adaptive beamforming for array imaging of plate structures using Lamb waves," *Ultrasonics, Ferroelectrics and Frequency Control, IEEE Transactions on* **57**, pp. 2712 –2724, december 2010.
5. P. Wilcox, "Omni-directional guided wave transducer arrays for the rapid inspection of large areas of plate structures," *Ultrasonics, Ferroelectrics and Frequency Control, IEEE Transactions on* **50**, pp. 699 –709, june 2003.
6. B. Yoo, A. S. Purekar, Y. Zhang, and D. J. Pines, "Piezoelectric-paint-based two-dimensional phased sensor arrays for structural health monitoring of thin panels," *Smart Materials and Structures* **19**(7), p. 075017, 2010.
7. S. Doctor, T. Hall, and L. Reid, "SAFT the evolution of a signal processing technology for ultrasonic testing," *NDT International* **19**(3), pp. 163 – 167, 1986.
8. R. Sicard, A. Chahbaz, and J. Goyette, "Guided lamb waves and l-saft processing technique for enhanced detection and imaging of corrosion defects in plates with small depth-to wavelength ratio," *Ultrasonics, Ferroelectrics and Frequency Control, IEEE Transactions on* **51**(10), pp. 1287–1297, 2004.
9. L. Moreau, B. Drinkwater, and P. Wilcox, "Ultrasonic imaging algorithms with limited transmission cycles for rapid nondestructive evaluation," *Ultrasonics, Ferroelectrics and Frequency Control, IEEE Transactions on* **56**, pp. 1932 –1944, september 2009.
10. M. Engholm and T. Stepinski, "Direction of arrival estimation of Lamb waves using circular arrays," *Structural Health Monitoring* , 2010.
11. L. Liu and F. G. Yuan, "A linear mapping technique for dispersion removal of Lamb waves," *Structural Health Monitoring* **9**, pp. 75–86, January 2010.
12. P. Wilcox, "A rapid signal processing technique to remove the effect of dispersion from guided wave signals," *Ultrasonics, Ferroelectrics and Frequency Control, IEEE Transactions on* **50**, pp. 419 –427, april 2003.
13. J. Davies, F. Simonetti, M. Lowe, and P. Cawley, "Review of synthetically focused guided wave imaging techniques with application to defect sizing," *AIP Conference Proceedings* **820**(1), pp. 142–149, 2006.
14. G. R. Lockwood, P.-C. Li, M. O´Donnell, and F. S. Foster, "Optimizing the radiation pattern of sparse periodic linear arrays," *IEEE Transactions On Ultrasonics, Ferroelectrics, and Frequency Control* **43**, January 1996.
15. L. Ambrozinski, *Advanced Structural Damage Detection: From Theory to Engineering Applications*, ch. Beamforming of guided waves, pp. 177–210. Wiley, 2013.
16. B. Xu and V. Giurgiutiu, "Single mode tuning effects on Lamb wave time reversal withpiezoelectric wafer active sensors for structural health monitoring," *Journal of Nondestructive Evaluation* **26**, pp. 123–134, 2007.
17. L. Ambrozinski, T. Stepinski, and T. Uhl, "Experimental comparison of 2D arrays topologies for SHM of planar structures," in *Nondestructive characterization for composite materials, aerospace engineering, civil infrastructure, and homeland security*, 2012.